

# S-BAND ELECTRON LINAC WITH BEAM ENERGY OF 30...100 MeV

*K.I. Antipov, M.I. Ayzatsky, Yu.I. Akchurin, V.A. Gurin, V.N. Boriskin, V.I. Beloglasov, E.Z. Biller, N.V. Demidov, A.N. Dovbnaya, R.N. Dronov, I.V. Khodak, A.I. Kosoy, V.A. Kushnir, V.A. Momot, L.K. Myakushko, V.V. Mytrochenko, T.F. Nikitina, A.N. Opanasenko, S.A. Perezhogin, G.D. Pugachev, O.A. Repikhov, L.V. Reprintzev, V.A. Shendrik, D.L. Stepin, G.E. Tarasov, Yu.D. Tur, V.F. Zhiglo*

*National Science Center "Kharkov Institute of Physics and Technology", Kharkov, Ukraine  
e-mail: mitvic@kipt.kharkov.ua*

The S-band electron linac has been designed at NSC KIPT to cover an energy range from 30 to 100 MeV. The linac consists of the injector based on evanescent oscillations and the two four-meter long piecewise homogeneous accelerating sections. Each section is supplied with RF power from the KIU-12AM klystron. Variation of mean energy of the beam over a wide range is produced by placing bunches out of the wave crest in the second accelerating section. The report presents layout of the linac as well as simulation results of self-consistent particle dynamics in the linac and its present status.

PACS: 41.75.Ht, 25.20.-x

## 1. INTRODUCTION

Recently, the growing interest to the researches employing photonuclear reactions on light nuclei is observed in the field of nuclear physics. To provide the researches, in particular, to refine cross-sections in such reactions, there it is required photon flux with fixed value of maximum energy. High-energy photon flux can be obtained with an electron accelerator whose beam energy can be varied in wide range of magnitudes. In this connection it has been decided to design research electron linac with wide beam energy variation that will be applied for the above purposes. The accelerator can be used also in the researches of numerous physical phenomena connected with interaction of relativistic electron beams with electrodynamic systems and condensed media. The results of the beam characteristics simulations, description of elements of the accelerator and its present status are given below.

## 2. SIMULATION

The choice of an accelerator structure was performed with the use of simulation results of self-consistent non stationary beam dynamics in traveling-wave accelerating structures obtained on the base of the technique described in [1]. Proceeding from the results of simulation and taking into account the NSC KIPT resources we decided to select the layout of the linac comprising two four-meter sections of the "Kharkov-85" type [2]. These sections are piecewise homogeneous disk loaded waveguides, consisting of four parts with a constant impedance. Each part is matched with the next

one with five matching cells. The total number of cells is 162, phase advance on the structure period is  $90^\circ$  and operating frequency is 2797.15 MHz. The values of the characteristics of the parts of the sections were calculated both by interpolation of the data from [3] and by the technique proposed in [4]. The both methods gave close results. Fig. 1 presents the calculated dependences of the group velocity related to the light velocity and attenuation as a function of the distance along the section. The calculated values of section filling time and attenuation were 0.92  $\mu\text{s}$  and 0.68 neper, respectively. The series impedances are equal to 1082, 1430, 1943 and 2930  $\text{Ohm}/\text{cm}^2$  for 1, 2, 3 and 4 subsections, respectively. Simulation has shown that with a power of 16 MW at the section entrances and 100 mA beam injection at particle energy of about 0.7 MeV, in the case of optimum phasing of the sections, the maximum energy gain will be 95 MeV taking into account the transients due to the filling time of the sections.

Changing the phase of the second section field created by the RF generator with an optimum selection of the injection moment, it is possible to obtain the necessary set of beam energies. Fig. 2 presents the beam energy spectrum plotted with taking into account the transient processes for different values of field phases in the second section.

The results obtained formed the basis of the method applied for beam energy control that will be used at the first stage of the investigations. The accelerator structure (see Fig. 3) was determined proceeding from the simulation data.

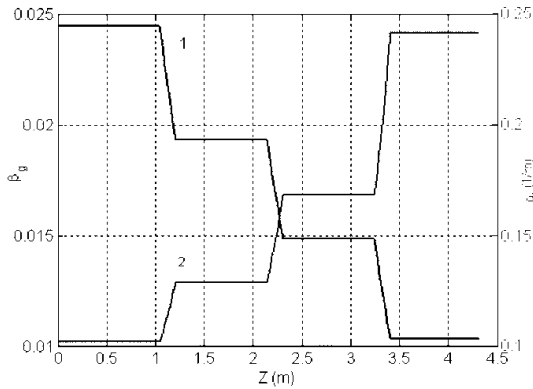


**Fig. 1.** Changing the group velocity related to the light velocity of light (1), and the attenuation (2) along the section

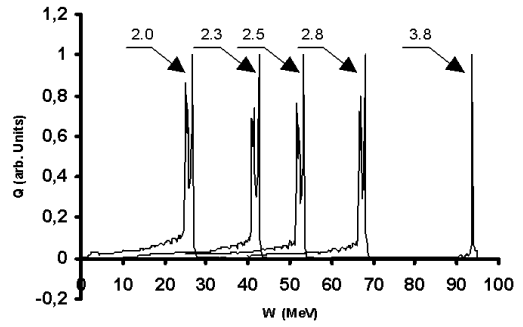


**Fig. 2.** Beam energy spectrum for different values of field phases in the second section (numerals at curves denote some phase shift in radians)

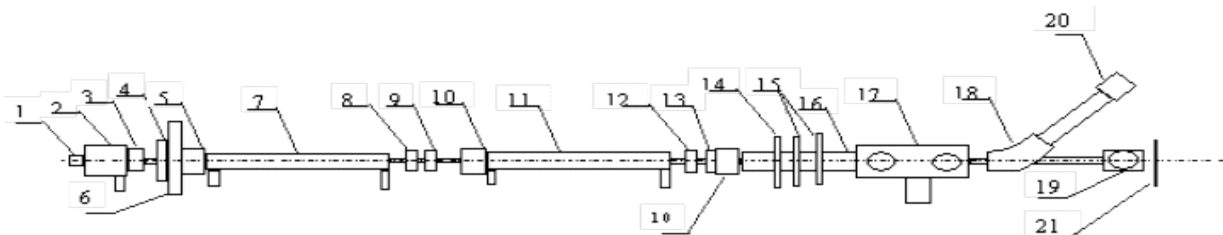


**Fig. 3.** Structural layout of the accelerator. 1 – electron gun, 2 – resonator system of the injector, 3, 9, 13 – current transformers, 4 – axial lens, 5, 10 – valves, 6 – adjustable collimator, 7, 11 – accelerating sections, 8, 12 – beam position monitors, 14, 15 – quadrupoles, 16 – beam pipe, 17 – unit of slot collimators and Faraday cup, 18 – magnetic analyzer, 19 – Faraday cup with an exit window, 20 – Faraday cup of the magnetic analyzer, 21 – tantalum converter

After finishing the injector tests [5] we have performed the simulation of particle dynamics in the whole accelerator by the technique, presented in [6]. This technique enabled to take into account the influence of space charge forces on the formation of bunches. The energy spread width of 1.5% for 70% of beam particles and the maximum energy at the exit of the second accelerating section of 95 MeV, with optimum phasing of sections, is in accordance with the data obtained by another technique [1]. The transverse normalized root-mean-square emittance ( $1\sigma$ ) in this case is  $15\pi$ -mmrad. When bunch is accelerating in the second section out of the wave crest, the FWHM energy spectrum is a few of percents, but long low-energy tails appear because the bunch phase length is not small.

The accelerator structure allows one to apply the other methods of energy beam control too. In particular, the preliminary calculations have shown that it is possible to obtain the required particle energy values due to the change of the injection current into the first section. To approve applicability of this method, it is necessary to carry out additional investigations since the beam current, required for this case, lies above the threshold current of the regenerative transverse instability in such sections [7].

The beam transport from the second section exit to the converter was calculated using the codes PARMELA [8] and TRACE3D [9].

### 3. DESCRIPTION OF THE ACCELERATOR

The accelerator comprises the following basic units and systems: injector; piecewise homogeneous accelerating sections; beam transport system; beam diagnostics system; RF power supply system; temperature control system; control system.

#### 3.1. INJECTOR

The injector (see Fig. 3) consists of a 25 kV diode gun and a bunching system based on evanescent oscillations [5]. In the standard operating mode the injector provides a current at the entrance into the first accelerating section up to 200 mA with the electron energy up to 1 MeV. The gun with a high perveance can be installed. In this case the current at the injector entrance can reach 1.2 A. The injector includes also a collimator providing the current control at the entrance into the accelerating section without changing conditions of bunch formation in the injector.

#### 3.2. ACCELERATING SECTIONS

The characteristics of accelerating sections are given above. The sections were operating in the structure of

the accelerator LUE 2 GeV [10]. Before installation on the accelerator being constructed the sections were tested. The measurements of the phase advance showed that at a mean phase wave velocity equal to the light velocity  $c$  the phase velocity in the first subsection of one of sections is  $0.9968c$ , and this value in the other section is  $0.9992c$ . Root-mean-square spreads of an error of phase advance per the cell of the sections were  $4.3^\circ$  and  $3.1^\circ$ . The measured and calculated values of attenuations in the sections coincide with an accuracy of 10%. The section with a less phase velocity in the first subsection was chosen as the first section.

### 3.3. BEAM TRANSPORT SYSTEM

The beam transport system includes an axial magnetic lens at the injector exit, steering coils along the sections, three quadrupoles and a steering magnet between the second section exit and the magnetic analyzer (the length of the drift is about 6 m). Magnetic elements are energized from the commercial power sources being controlled by the control system.

### 3.4. BEAM DIAGNOSTICS SYSTEM

The beam diagnostics system comprises the inductive beam current transformers at the exits of the injector and accelerating sections, the inductive four-winding beam position monitors at the exit of sections, the Faraday cup and the magnetic analyzer of beam energy. The magnetic analyzer is provided with a dipole magnet having the bending angle of  $25^\circ$ . The angles of the magnet faces and the distance from the magnet to the analyzing slit were chosen as a result of calculations with the use of the code TRACE 3D. The energy resolution of the analyzer is 0.2%.

### 3.5. RF POWER SUPPLY SYSTEM

The RF power supply system of the accelerator consists of the two KIU12AM klystrons providing the maximum pulse power up to 20 MW at a pulse duration of 2.5  $\mu$ s and pulse repetition rate of 50 pps. The second klystron is exited via the directional coupler installed in the RF feeder of the first section and the fast phase shifter. The phase shifter is controlled by the accelerator control system that allows one to perform computer controlling of the beam energy. In the same place the directional coupler with a minimum attenuation of 10.3 dB is installed for power supply to the injector. The first klystron works in the mode of a self-excited oscillator with a stabilizing resonator in the feedback circuit.

### 3.6. TEMPERATURE CONTROL SYSTEM

The temperature control system of the accelerator provides thermal stabilization of the two accelerating sections and the injector. The system comprises 7 temperature-sensitive elements, 8 transducers of water flow through the objects being cooled and 2 water pressure pickups. For analysis of signals from the transducers and for temperature control the microprocessor complex ADAM 5011 and the commercial thyristor controllers are used. Information

of the process parameters is displayed on the local control desk, as well as, via the RS-485 port is transferred to the accelerator control room.

### 3.7. CONTROL SYSTEM

To control the accelerator operation the automatic control system was developed providing the control of the current, energy and electron beam position, control of parameters of accelerator systems, interlocking of the modulator and the klystron amplifier under impermissible operating conditions, control of currents in the power sources of the beam guide, control of phase and power of RF-signal in the injection system. The software-hardware complex comprises the PC with a crate KAMAK having the fast four-channel ADP, synchronization unit, microprocessor control complexes regulating the operation of the temperature control system and the magnet current sources.

### 4. CURRENT STATUS

Currently the basic accelerator systems are installed and adjusted. The injector is tested on the special stand and in the near future it will be mounted on the accelerator. In the accelerating sections and in the electron guide the working vacuum is obtained.

### 5. CONCLUSIONS

The S-band electron linac has been designed at NSC KIPT to cover an energy range from 30 to about of 100 MeV, the main purpose of which is generation of photon fluxes with fixed maximum energy. The accelerator structure allows one to apply different schemes of beam energy variation. The calculated characteristics of the beam in the mode with a maximum energy gain, in particular, a normalized emittance not exceeding  $15 \pi$ -mm-mrad, make it possible to apply this accelerator also for the researches of numerous physical phenomena related to interaction of relativistic electron beams with electrodynamic systems and condensed media.

### REFERENCES

1. M.I. Ayzatsky. *Nonstationary Model for Beam Dynamic Simulation in Multisectional Accelerators*. Proc. of the EPAC98, Stockholm, 1998, p. 1159-1161
2. E.Z. Biller, et al. Beam Current Enhancement in Kharkov Electron Linac // *Part. Accel.* 27, 1990, p. 119-124.
3. O.A. Valdner, N.P. Sobenin, B.V. Zverev, I.S. Shchedrin. *Disk loaded waveguides: Reference book*. M.: "Ehnergoizdat", 1991, 280 p. (in Russian).
4. G.A. Loew, R.H. Miller, R.A. Early, and K.L. Bane. Computer Calculations of traveling wave periodic structure properties // *IEEE Trans. Nucl. Sci.* NS-26, 1979, p. 3701.
5. M.I. Ayzatsky, E.Z. Biller, K.Yu. Kramarenko et al. *Test Results of Injector Based on Resonance System*

- with Evanescent Oscillations*, Abstracts of the EPAC04, Lucerne, 2004, p. 74.
6. V.V. Mytrochenko, A.N. Opanasenko. *Simulation Technique for Study of Transient Self-Consistent Beam Dynamics in RF Linacs* Abstracts of the EPAC04, Lucerne, 2004, p. 159.
  7. A.N. Dovbnya, L.M. Zavada, A.I. Zykov, et al. Experimental research of transversal instability of a bunch in single accelerating sections // *Vorposy Atomnoj Nauki I Tekhniki, Ser.: Yaderno-Fizicheskiye Issledovaniya*. 1989, №6(6), p. 46-50 (in Russian).
  8. L.M. Young. *PARMELA*, Los Alamos, Preprint LANL, LA-UR-96-1835, 1996, 108 p.
  9. K.R. Crandall, D.P. Rusthoi. *TRACE 3-D Documentation*, Los Alamos, Preprint LANL, LA-UR-97-886, 1997, 115 p.
  10. J. Clendenin, L. Rinolfi, K. Takata, D.J. Warner, *Compendium of Scientific Linacs*, Proc. of the LINAC96, Geneva, Switzerland, August 1996, p. 175.

### **ЛИНЕЙНЫЙ УСКОРИТЕЛЬ ЭЛЕКТРОНОВ 10 см - ДИАПАЗОНА С ЭНЕРГИЕЙ ПУЧКА 30...100 МэВ**

*К.И. Антипов, Н.И. Айзацкий, Ю.И. Акчурин, В.А. Гурин, В.Н. Борискин, В.И. Белоглазов, Е.З. Биллер, Н.В. Демидов, А.Н. Добня, Р.Н. Дронов, И.В. Ходак, А.И. Косой, В.А. Кушнир, В.А. Момот, Л.К. Мякушко, В.В. Митроченко, Т.Ф. Никитина, А.Н. Опанасенко, С.А. Пережогин, Г.Д. Пугачев, О.А. Репихов, Л.В. Репринцев, В.А. Шендрік, Д.Л. Степин, Г.Е. Тарасов, Ю.Д. Тур, В.Ф. Жигло*

Линейный ускоритель электронов 10 см - диапазона был разработан в ННЦ ХФТИ с целью перекрытия диапазона энергий 30...100 МэВ. Ускоритель состоит из инжектора, основанного на не распространяющихся колебаниях и двух кусочно-однородных четырехметровых ускоряющих секций. Каждая секция питается СВЧ-мощностью от клистрона КИУ-12АМ. Изменение средней энергии пучка в широких пределах обеспечивается ускорением сгустков не на гребне волны во второй ускоряющей секции. Представлены структурная схема ускорителя, результаты моделирования динамики частиц в ускорителе и его текущее состояние.

### **ЛІНІЙНИЙ ПРИСКОРЮВАЧ ЕЛЕКТРОНІВ 10 см - ДІАПАЗОНУ З ЕНЕРГІЄЮ ПУЧКА 30...100 МеВ**

*К.І. Антипов, М.І. Айзацький, Ю.І. Акчурін, В.О. Гурін, В.М. Борискін, В.І. Белоглазов, Е.З. Біллер, М.В. Демідов, А.М. Добня, Р.М. Дронов, І.В. Ходак, А.І. Косой, В.А. Кушнір, В.О. Момот, Л.К. Мякушко, В.В. Митроченко, Т.Ф. Нікітіна, А.М. Опанасенко, С.О. Пережогін, Г.Д. Пугачев, О.О. Репіхов, Л.В. Репрінцев, В.А. Шендрік, Д.Л. Стєпін, Г.Є. Тарасов, Ю.Д. Тур, В.Ф. Жигло*

Лінійний прискорювач електронів 10 см - діапазону було розроблено в ННЦ ХФТІ з метою перекрити діапазон енергій 30...100 МеВ. Прискорювач складається з інжектора, основаного на коливаннях, що не розповсюджуються, і двох шматково-однорідних чотириметрових прискорювальних секцій. Кожна секція забезпечується НВЧ-потужністю від клістрона КІУ-12АМ. Зміна середньої енергії пучка в широких межах забезпечується прискоренням згустків не на гребені хвилі в другій прискорювальній секції. Представлено структурну схему прискорювача, результати моделювання динаміки частинок в прискорювачі і його поточний стан.